ISOLATION AND CHARACTERIZATION OF MICROCRYSTALLINE CELLULOSE FROM OIL PALM FRONDS USING CHEMOMECHANICAL PROCESS

Abdulwahab F. Owolabi

Researcher
School of Industrial Technology
Universiti Sains Malaysia
11800 Penang, Malaysia
Federal Institute of Industrial Research Oshodi
Lagos, Nigeria
E-mail: fathok2375@gmail.com

Arniza Ghazali

Senior Lecturer
E-mail: arniza@usm.my

H. P. S. Abdul Khalil

Professor
School of Industrial Technology
Universiti Sains Malaysia
11800 Penang, Malaysia
E-mail: akhalilhps@gmail.com

Azman Hassan

Professor
E-mail: azmanh@cheme.utm.my

Reza Arjmandi

Post Doctoral Fellow
Department of Bioprocess and Polymer Engineering
Faculty of Chemical and Energy Engineering
Universiti Teknologi Malaysia
Johor Bahru Skudai, Malaysia
E-mail: reza_arjmandi@usm.my

M. R. Nurul Fazita

Senior Lecturer
E-mail: fazita@usm.my

*M. K. Mohamad Haafiz**

Senior Lecturer
School of Industrial Technology
Universiti Sains Malaysia
11800 Penang, Malaysia
E-mail: mhaafiz@usm.my

(Received June 2016)

* Corresponding author

Abstract. This study investigates the characteristic of the microcrystalline cellulose (MCC) isolated from oil palm (*Elaeis guineensis*) fronds using acid hydrolysis method. The morphology and size of the MCC were characterized using both Scherrer equations for X-ray diffraction (XRD) result and transmission electron microscopy. The thermal stability of MCC was determined from thermogravimetric analysis (TGA) profiles, whereas Fourier transform IR (FTIR) spectroscopy was used to analyze the chemical modifications that occurred under these conditions. The XRD results showed that the MCC isolated from oil palm fronds (OPF-MCC) fibers had an average diameter and crystallinity index of 12.15 nm and 60.1%, respectively. Both FTIR spectroscopy and XRD indicated that lignin and hemicellulose contents decreased, whereas the cellulose-I polymorph remained constant. TGA revealed that OPF-MCC had higher thermal stability compared with the OPF fibers. The study revealed the potential applications of the MCC isolated from the oil palm biomass as green reinforcement and/or fillers in the production of biodegradable biocomposite.

Keywords: Oil palm fronds, microcrystalline cellulose, acid hydrolysis, biocomposite, transmission electron microgram.

INTRODUCTION

Over the last decade, there has been growing interest of researchers in the use of natural fibers (mineral fibers, animal fibers, vegetative fibers) in polymer composites reinforcement. Of all the classes of natural fibers, vegetative fibers (cotton, jute, flax, ramie, sisal, hemp, etc.) have been reported used in polymer composite reinforcement because of relatively low density (Poletto et al 2010). Properties that influences the use of vegetative fibers include, relatively stiff and strength, natural fibers cellulose have gained wide acceptability as fillers in polymer composite (Kalia et al 2014). A wide variety of different natural fibers which can be applied as reinforcers or fillers consist of elongated cells with relatively thick cell walls which make them stiff and strong. Application of natural fibers in composite reinforcement has been widely accepted because of their: renewability, economical, biodegradability, health advantages, and recyclability (Hollaway 2010; Bhatia et al 2016; Zimniewska and Wladyka-Przybylak 2016). In automobile industries where weight reduction is always an issue, natural fibers are applied for most of the interior parts because of their high specific modulus. As a result of the economic advantage, replacement of glass fibers with natural fiber–reinforced composites are originally proposed. Health hazards such as skin irritation, eye hitching, and lung cancer are prevented from the composite producers with the use of natural fibers (Sanyang et al 2016).

In tropical countries like Malaysia, oil palm fronds (OPF) are one of the main by-products of the cultivation of oil palm trees (*Elaeis guineensis* Jacq.) in oil palm industries. OPF is available all year round because it is obtained during pruning, harvesting, or replanting. The large quantity of fronds produced by a plantation each year makes this biomass very abundant (Awalludin et al 2015). Majorly both OPF and oil palm trunk are residues available in the oil palm plantations. The total global oil palm harvested from 15 million ha in 2009 (FAO et al 2011) generated about 164 million tons dry matter (DM) of OPF (FAO et al 2011). In Malaysia, 26 million metric tonnes DM of OPF are produced annually during pruning. Chan et al (1980) reported that about 24 fronds are pruned per palm tree annually, and the weight of fronds varies considerably with age of the palm, with an average annual pruning of 82.5 kg of fronds/palm/year (Zahari et al 2003; Sulaiman et al 2012). Most of the OPF are left rotting between the rows of palm trees, mainly for soil conservation, erosion control, and ultimately for the long-term benefit of nutrient recycling. The chemical analysis of the OPF shows that the biomass is rich in cellulose which make (99.7% [w/w]) were purchased from Sigma-Aldrich Co. (St. Louis, MO) it suitable as raw material for

biodegradable reinforcement and green fillers in polymer composite (Khalil et al 2007; Khalil et al 2012). The recent global growing interest in research and development of greener technologies have thrown lights into the use of abundant agricultural biomass composite formulation (Pandey et al 2015). Plant fibers have been reported to be used as reinforcement in plastics composite industry in place of inorganic and synthetic fibers like clay, glass, aramid, etc. (Fiore et al 2015; Jagadeesh et al 2015). Many varieties of plant fibers used for this purpose exist, they include plants fibers such as cotton, kapok, flax, hemp, jute, ramie, sisal, henequen, and coir, including empty fruit bunches (EFB) that was recently reported as inclusion in the array of the lignocellulose biomass. By far, the most abundant are the wood fibers from trees; however, other fiber types are emergent in use (Bajpai 2015; Gurunathan et al 2015).

Microcrystalline cellulose (MCC) is an odorless, tasteless, white powder, and moderately depolymerized cellulose prepared from α-cellulose by acid hydrolysis. Battista et al in the 1950s pioneered the research work on MCC studies that has led to the commercial production of MCC. Basically, mineral acid hydrolysis of α-cellulose from lignocellulose materials leads to dissolution of the amorphous region of the cellulose chains while leaving the crystalline part intact. The MCCs are generally insoluble in water, dilute acid, and most organic solvents. MCC has gained wide acceptability in industries especially the pharmaceutical industry as an inactive binder in drug tablets. In addition, MCC is widely used in fat-free food additives and suspension stabilizers in the food and cosmetic industries. Depending on geography location, wood is sometimes the most abundant resources for commercial production of MCC. Because of the increased cost of production occasioned by the scarcity of wood that is the major source of commercial MCC, research studies on preparing MCC from lignocellulose biomass has been growing (Ibrahim et al 2013). Utilization of wood and agricultural products depends on its fiber crystallinity because of the influence of the fiber crystallinity on their physical, mechanical, and chemical properties. It was reported that while the increase in the fiber crystallinity enhances the properties such as tensile strength, dimensional stability, and density, increment in the fiber crystallinity reduces properties such as chemical reactivity and fiber swelling. Among the frequently used techniques for estimating cellulose crystallinity are X-ray diffraction (XRD), solid state 13C cross-polarization/magic-angle spinning, nuclear magnetic resonance spectroscopy, Fourier transform IR (FTIR) spectroscopy, near-IR FT Raman, and sum frequency generation vibration spectroscopy (Agarwal et al 2012). The use of lignocellulose biomass such as wheat straw (Alemdar and Sain 2008), rice straw and baggase (Ilindra and Dhake 2008), and of recent EFB (Haafiz et al 2013; Mdh et al 2015) as fillers or reinforces in polymer composite has been reported. Some of the properties of MCC obtained from lignocellulose biomasses have been reported comparable with those used commercially in various industries. Growing interest on the use of MCC powder in production of cellulose nanocrystals because of its particulate nature has also been reported (Zeni et al 2016).

The abundance of the raw material is also a concern to the manufacturing industry, and the pressures on it to use evermore "greener" technologies have made this area of research of worldwide interest. Oil palm waste has been reported as natural cellulose fibers containing high cellulose, hence will significantly benefit agricultural use, fiber resource, food, and energy needs (Ramesh 2016; Tye et al 2016). The conversion of all this biomass to products useful in composite will help the environment because the products are considered as sustainable green materials. Also, this application will tackle the problem of oil palm waste being left out in the field or burned, hence contributing to the economy by turning it into valuable products. Despite the report that wood, cotton, and many lignocellulose biomass have been major sources of MCC, but because of sustainability, industrial ecology and eco-efficiency, renewed and growing interest in the search for alternative source of cellulosic raw materials has been intensified. The high cellulose content of

55.54% (Owolabi et al 2016) in OPF represents a vast potential that could be exploited for high value-added products via conversion into cellulose derivatives, such as MCC which is the aim of this investigation.

To the best of our knowledge, isolation and characterization of MCC from OPF vascular bundles has not been previously reported. The objective of present study is to isolate MCC from OPF fiber using hydrochloric acid hydrolysis for future use as green filler in biocomposite manufacture. The isolated MCC was characterized with respect to the morphology, thermal, crystallinity index.

MATERIALS AND METHODS

Materials

OPF was supplied from oil palm plantation Pulau Pinang, Malaysia. The supplied OPF was cut into about 2 cm and with the aid of a Willey Mill was milled and sieved to 500 μm. the chemicals including sodium hydroxide (NaOH) (97% [w/w]), hydrogen peroxide (H_2O_2) (30% [w/w]), hydrochloric acid (HCl) (37% ACS reagent), sodium chlorite ($NaClO_2$) (80% [w/w]), and acetic acid (CH_3COOH) (99.7% [w/w]) were purchased from Sigma Aldrich Co. and used without further purification.

Extraction of Cellulose Fiber from OPF

The prepared OPF powder was first prehydrolyzed with water at 70°C for 30 min and drained to evacuate the water soluble extractives. The fiber was then subjected to alkaline hydrogen peroxide at the hydrogen peroxide to alkali ratio of (2.5:2.0 w/v H_2O_2:NaOH) treatment for 30 min followed by mechanical refining with laboratory Buah refiner (Owolabi et al 2016). The pulp slurry was washed screened and dried to determine the yield. The obtained pulp is further bleached using a totally chlorine-free sequences of oxygen (O), peroxide (P) and per acetic acid prepared in situ as described by Behin et al (2008) with modification. The bleached OPF extracted fiber was washed thoroughly before the acid hydrolysis.

Extraction of MCC from the Bleached OPF Fiber

MCC from the bleached OPF fiber was prepared according to the method described by (Haafiz et al 2013) based on original procedures described by (Battista 1950) with a slight modification. In brief, 30 g of the obtained bleached OPF pulp was hydrolyzed with 13 mL·g^{-1} of 37% HCl (w/w) with the acid hydrolysis carried out at a solid-liquor ratio of 1:20 with refluxing at $105 \pm 2°C$ under constant agitation for 30 min. After the acid hydrolysis, the dispersed pulp slurry was washed and made three cycles of centrifugation at 10,000 rpm. The final wash was done by dialysis in membrane of regenerated cellulose with distilled water for 72 h until the pH achieves neutrality and the residue obtained was filtered before air dried. The powder OPF-MCC sample was obtained by grinding the air-dried sample in a ball mill and subsequently kept in a desiccator.

Characterization of MCC

Transform IR spectroscopy analysis. The chemical changes on the isolated OPF-MCC occasioned by the chemical treatment were monitored using FTIR spectroscopy. The sample was pelletized with KBr in the ratio of 1:100. The pelletized sample was run on spectra analysis performed on a Perkin Elmer 1600 IR spectrometer FTIR spectra of a Nicolet AVATAR 360 at 32 scans (Perkin-Elmer, Foster City, CA) with a resolution of 4 cm^{-1} and within the wave number range of 400-4000 cm^{-1}.

Morphological Analysis

Field emission scanning electron microscopy. Field-emission scanning electron microscope (FESEM) was used to monitor the surface morphological transformations of the OPF-MCC sample. The analysis which were studied on LEO Supra 50 Vp, were sputter-coated with

gold to avoid charging. The OPF-MCC were placed on gold-sputtered coater model Polaron SC 515 ± 20 nm and then projected on audio-visual display unit.

Transmission electron microscopy. Transmission electron microscopy (TEM) was used to view and measure the structural dimension of the OPF–MCC using a Philips CM 12 electron microscope with an accelerating voltage of 80 kV. The OPF-MCC specimens were sonicated and stained with a drop of 2% uranyl acetate to improve the viewing contrast. The dispersed OPF-MCC samples were dropped on copper grids coated with a carbon support film for observation. The result of 20 OPF-MCC fibers was reported as the mean value of the data from each set of measurements.

Thermogravimetric Analysis

Thermogravimetric analyser, model Perkin-Elmer TGA 7 was used to monitor the changes in weight when the specimens were scanned from 30°C to 800°C at a rate of 10°C min^{-1} under a nitrogen gas atmosphere. The thermal stability data of OPF-MCC samples were collected and reported.

XRD Analysis

The cellulose crystallinity of the OPF-MCC was monitored using X-ray diffractometer with Ni-filtered CuKα radiation (wavelength of 1.5406 A). The operating voltage of the diffractometer was 40 kV voltage and current of 40 mA. The test samples were scanned within a 2θ angle range from 5° to 60° at 2°/min with the operating voltage of diffractometer of 40 KV and 40 mA current. The crystallinity index value was calculated according to Segal et al (1959), Eq (1):

$$\text{Crl}(\%) = \frac{(I_{002} - I_{am})}{I_{002}} \times 100 \qquad (1)$$

where I_{002} and I_{am} are the peaks intensity corresponding to crystalline and the amorphous fraction, respectively.

The average crystallite size was calculated from the Scherrer Eq (2) based on the width of the diffraction patterns obtained in the X-ray reflected the crystalline region.

$$D_{002} = \frac{k\lambda}{B_{002}\cos\theta} \qquad (2)$$

where k is the Scherrer constant (0.84), λ is the X-ray wavelength (1.54 nm), B in radians is the full width at half of the peak an FWHM to 9.5mm of 002 diffraction peak, and θ the corresponding Bragg angle.

RESULTS AND DISCUSSION

Thermal Properties

The result of the thermogravimetric analysis (TGA) of the raw OPF and OPF-MCC samples are shown in Fig 1 whereas the derivative thermogravimetric (DTG) curves are shown in Fig 2. The summary of the various temperatures at the corresponding weight loss is shown in Table 1. The original weight loss of about 5% did not involve thermal degradation of the MCC, but rather is the removal of MCC, and was found to occur between 25°C to about 105°C. This small weight loss is characteristic of moisture removal caused by evaporation of loosely bound moisture on the surface of the sample (Poletto et al 2010; French 2014). As shown in Fig 1, the raw OPF sample initiates a slightly more pronounced degradation process from 245°C, whereas the more prominent degradation observed at 290°C as shown in Fig 2 is because of hemicellulose degradation (Nagalakshmaiah et al 2016) in the raw sample. The onset temperature for the raw OPF (245.73°C) lower than the OPF-MCC (313.19°C) could be attributable to the presence of amorphous materials in the raw sample that degraded early. The maximum thermal diminution for the raw and the OPF-MCC were 341.38°C and 345.23°C, respectively, corresponding to cellulose degradation (Jonoobi et al 2012). The cellulose diminution stage is occasioned by the glycosidic bond cleavage resulting
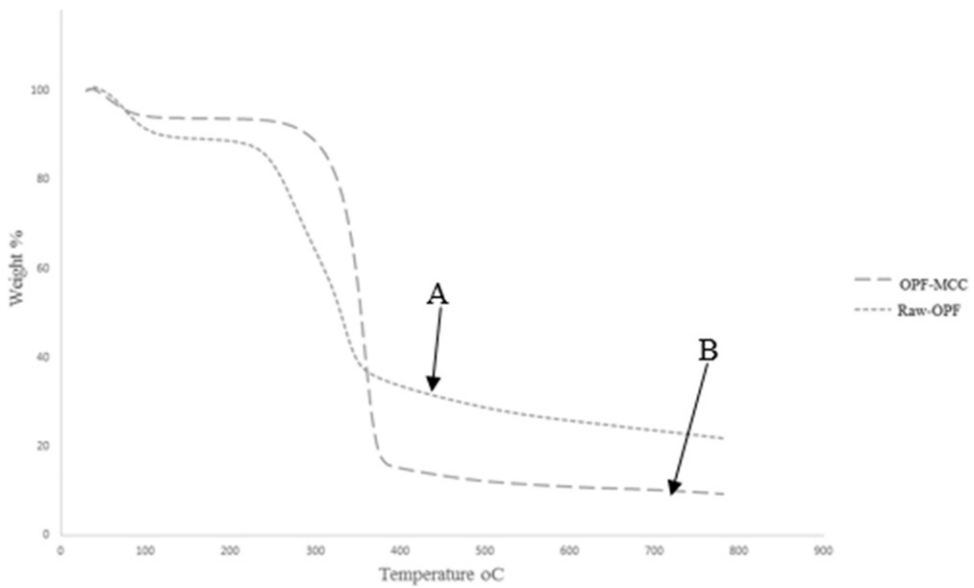
Figure 1.   Thermogravimetric analysis curves of (A) raw oil palm fronds (OPF) fiber and (B) OPF–microcrystalline cellulose.

in the depolymerization of the polymer to the formation of CO_2, H_2O couple with the formation of variety of hydrocarbon derivatives (Poletto et al 2010).

Generally, the chemomechanical treatment and the acid hydrolysis, the thermal stability and degree of crystallinity of the lignocellulosic materials due to the removal of hemicelluloses
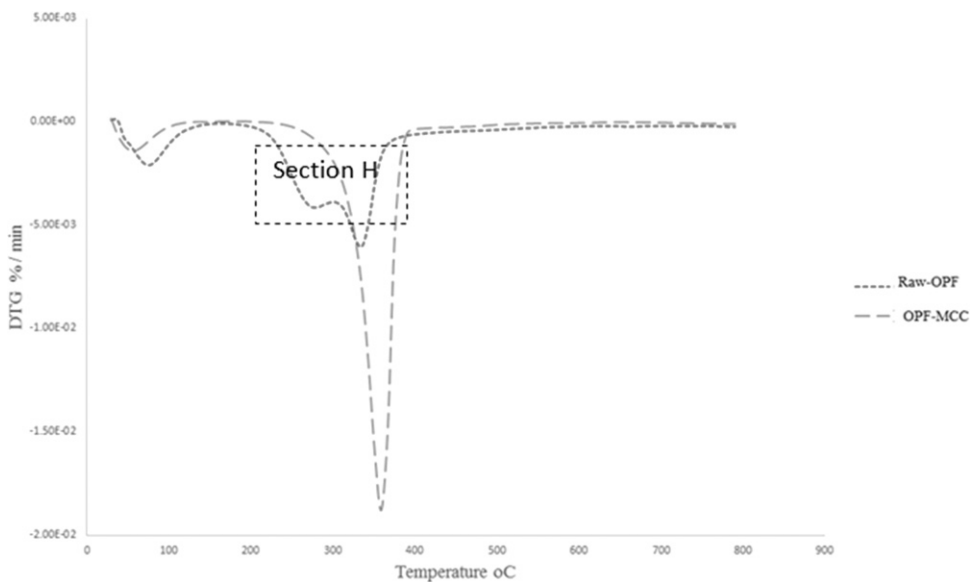
Figure 2.   Derivative Thermogravimetric analysis DTA curves of (A) raw oil palm fronds (OPF) fiber and (B) OPF–microcrystalline cellulose (MCC).

Table 1. Thermal properties of the tested samples.

Sample	$T_{(onset)}$	$T_{(20\%)}$	$T_{(max)}$	Residue %
OPF-MCC	313.19°C	327.67°C	345.23°C	13.11
OPF-Raw	245.73°C	257.17°C	341.38°C	22.47

OPF, oil palm fronds; MCC, microcrystalline cellulose.

reinforcement and lignin. OPF-MCC has a higher decomposition peaks of 345°C than oil palm empty fruit bunches (OPEFB)–MCC (326 °C) as reported by Haafiz et al (2013) and jute (316°C) as reported by Johar et al (2012). Although the former could be attributable to the effect of the alkaline hydrogen peroxide prehydrolysis, the latter is because of the introduction of sulfate groups into the outer surface of the jute cellulose crystals during hydrolysis.

Further heating of the samples beyond 400°C showed that raw OPF and OPF-MCC had degraded by 70% and 85%, respectively. The residual char obtained at the end of the heating exercise were found to be higher in the raw-OPF (22.47%) sample than the OPF-MCC (13.11%). The formed char was ascribed to the combination of the residual lignin and ash in the samples (Rosa et al 2012; Sonia and Dasan 2013). The low residual char recorded in the OPF-MCC is attributable to the effect of the acid hydrolysis through the removal of the amorphous part of the crystalline cellulose (Habibi et al 2010;

Mdh et al 2015). With high crystallinity index and thermal stability, OPF-MCC is considered suitable for green biocomposite production.

Field Emission Scanning Electron Microscopy

The structural transformation of the prepared OPF-MCC was monitored through FESEM. As shown in the FESEM image, Fig 3a represents the image of the OPF raw fiber, whereas Fig 3b represents the image of OPF-MCC. The image is characterized with unseparated fiber bundles with the fibers stick together with traces of craters. The FESEM micrographs in Fig 3b represents the image of the OPF-MCC fibers. The image reveals separated fibers indicating the removal of the cementing amorphous substances such as the hemicelluloses, lignin, and pectin present in the raw OPF sample as a result of the alkaline hydrogen peroxide AHP pretreatment, bleaching, and hydrolysis. The FESEM image revealed fragmented smooth-walled separated fiber.

Transmission Electron Microscopy

TEM micrographs of the acid-hydrolyzed MCC is shown in Fig 4. The image revealed that after the acid hydrolysis, the isolated fiber undergoes
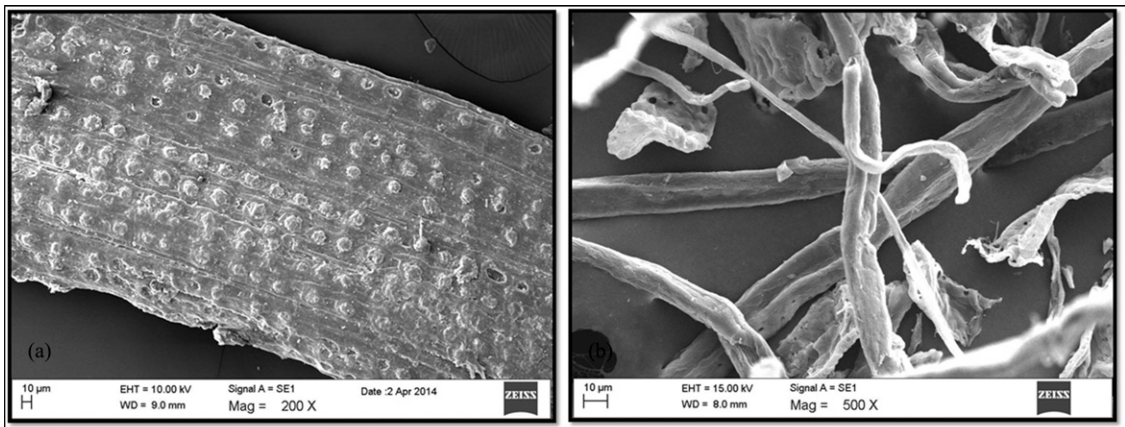
Figure 3. Field-emission scanning electron microscope images of (a) raw oil palm fronds (OPF) ×200 and (b) OPF–microcrystalline cellulose at ×500 magnification.
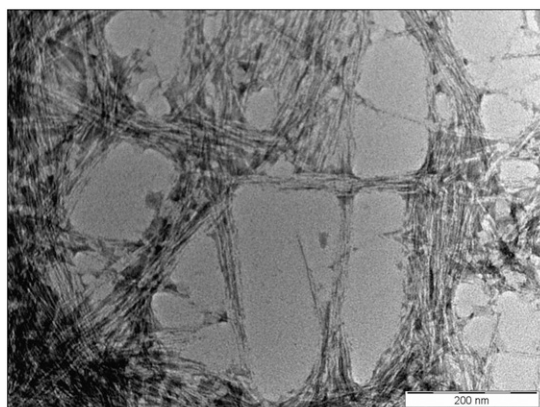
Figure 4.   Transmission electron microscope images of the oil palm fronds–microcrystalline cellulose.

Figure 5.   X-ray diffraction patterns of (a) raw oil palm fronds (OPF) and (b) acid-hydrolyzed OPF.

transverse cleavage of the amorphous region of the microfibrils. This fragmentation in the cellulose structure further incurred reduction in size with the further breakage of the glycosidic bond between the adjacent fibers. The TEM image gave individual fibers of average fiber diameter of 13.35 ± 0.47 nm. The fiber length was still observed unchanged at the micron scale despite the acid hydrolysis, which agrees with the result reported in the literatures (Azizi Samir et al 2005; Johar et al 2012).

XRD of Sample

The effectiveness of the acid hydrolysis was monitored with the determination of the crystallinity index (Crl) (Fig 5). The XRD pattern gave a monoclinic sphenodic structure characteristic of cellulose-1 polymorph. The similarity in the two XRD patterns in Fig 5 shows that the treatment of the raw biomass does not affect the natural cellulose-1 polymorph structure of the biomass. Table 1 gives the summary of the values of the crystalline index and crystalline sizes of the materials. The crystalline cellulose was determined through the crystallinity index which indicates that the crystallinity of the fiber increased with the treatment of the raw OPF. The crystalline size depicts the values obtained from the Scherrer equation. Although crystallinity of a material depends on the raw bio-

mass sources and the treatment, from Table 2, the crystallinity of the biomass increased with the chemical treatment. Crystallinity index of the MCC from the OPF was 60%, which is lower from the value obtained for eucalyptus (74.66%) (Zeni et al 2016), OPEFB-pulp (80%), OPEFB-MCC (87%), and commercial C-MCC (79%) (Haafiz et al 2013). The crystallinity sizes increases with the acid hydrolysis, which reaffirms the removal of the noncellulosic amorphous portion of the cellulose structure with acid hydrolysis. There is a slight difference in the crystalline size obtained from the Scherrer equation and the direct measurement from the TEM. The observed difference is attributable to the thermal vibration of a lattice site in crystalline structure as explained by Debye-Scherrer thermal broadening (Lionetto et al 2012).

Fourier Transform IR Spectroscopy

The chemical modifications in the cellulose structure after the chemical treatment of the raw biomass was monitored with the aid of FTIR

Table 2.   Crystallinity index and size of the microcrystalline cellulose from OPF.

	Crystallinity index	Crystalline size (Scherrer equation)
OPF-MCC	60.1%	12.15 nm
Raw OPF	38.0%	7.28 nm

OPF, oil palm fronds; MCC, microcrystalline cellulose.

spectroscopy. The FITR spectra of raw OPF and OPF-MCC were presented in Fig 6 indicating prominent spectra absorption peaks, whereas the vibrational assignments are summarized in Table 3.

The similarities of the peaks at the functional group with insignificant differences in the fingerprint section confirms the stability of the cellulose-1 polymorphs of the raw biomass despite the chemical treatments as equally shown in the XRD pattern. From Fig 6, the broad peak 3300 and 3400 cm^{-1} of the raw OPF and the OPF-MCC, respectively, is ascribed to the stretching vibration of O-H (hydroxyl) groups. The peak at 2900 and 2928 cm^{-1} of the two samples investigated are attributed to C-H stretching of cellulose (Elazzouzi-Hafraoui et al 2007). Comparison of the spectra at the fingerprint region shows some slight shift coupled with the appearance and disappearance of peaks. The disappearance of the peak 1735 cm^{-1} present in the raw OPF in the OPF-MCC characteristic of

C=O stretching is ascribed to unconjugated carbonyl group of the acetyl groups typical of hemicellulose and further stress the hemicellulose and lignin removal during the chemical treatment (Adel et al 2010). This band is observed to disappear in MCC, which is in agreement with the DTG result (Section H). The presence the peak at 1640 cm^{-1} which becomes prominent after the acid treatment is attributable to the bending mode of the absorbed water. This observation is similar to the result of the hydrochloric hydrolysis of OPEFB as reported by Haafiz et al (2014). Another prominent spectra peak of interest at the fingerprint region are 1317 cm^{-1} and 879 cm^{-1} ascribed to CH_2 wagging stretch and glycosidic bond, respectively. The peaks are characteristic cellulose-1 polymorph crystals of the OPF-MCC (Habibi et al 2010; Lionetto et al 2012).

CONCLUSIONS

The study revealed the successful isolation of OPF-MCC from waste OPF biomass, which is
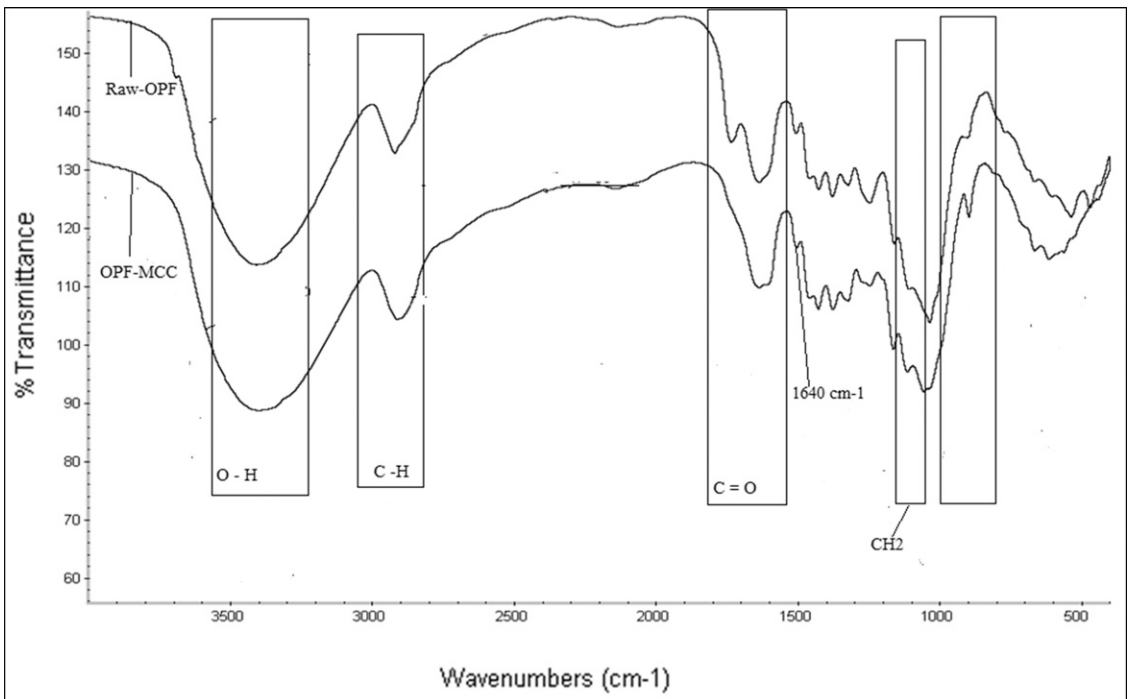
Figure 6.   Fourier transform IR spectra obtained from (a) raw oil palm fronds (OPF), and (b) OPF–microcrystalline cellulose.

Table 3. Summary of the FTIR spectra analysis of the two biomass.

Wavelength		Functional groups	Assignment
Raw OPF	OPF-MCC		
3300 cm^{-1}	3400 cm^{-1}	O-H groups	Hydroxyl in cellulose
2900 cm^{-1}	2928 cm^{-1}	C-H stretching	Cellulose
1723 cm^{-1}	—	C=O stretching	Hemicelluloses/lignin
1640 cm^{-1}	1640 cm^{-1}		
1510 cm^{-1}	1426 cm^{-1}	C-C stretching vibrations	Aromatic hydrocarbons of lignin
—	1317 cm^{-1}	CH$_2$ wagging	Cellulose (crystalline) 1
897 cm^{-1}	897 cm^{-1}	Asym. out of phase ring stretching	β-Glycosidic linkage of cellulose

FTIR, Fourier transform IR; OPF, oil palm fronds; MCC, microcrystalline cellulose.

one of the most abundant biomass from oil plantation in Malaysia yet to attract industrial advantage. The value of the diameter of the OPF-MCC from TEM analysis is 13.35 ± 0.47 nm, which is different from 12.15 nm obtained from the Scherrer equation. This is attributable to the thermal vibration of a lattice site in OPF-MCC crystalline structure. The results of the OPF-MCC characterization revealed an improvement in the thermal stability, increased crystallinity, and stability of the cellulose-1 polymorphs. The effective reduction in the lignin content of the OPF-MCC compared with the raw is exemplified by the low char obtained from the char residue of the thermal degradation of the OPF-MCC compared with the value obtained from raw OPF biomass. The high thermal stability couple with the improved crystallinity qualifies the OPF-MCC as a potential material for reinforcing green material in biocomposite formulation.

REFERENCES

Adel AM, El-Wahab ZHA, Ibrahim AA, Al-Shemy MT (2010) Characterization of microcrystalline cellulose prepared from lignocellulosic materials. Part I. Acid catalyzed hydrolysis. Biores Technol 101:4446-4455.

Agarwal UP, Reiner RR, Ralph SA (2012) Estimation of cellulose crystallinity of lignocelluloses using near-IR FT-Raman spectroscopy and comparison of the Raman and Segal-WAXS methods. J Agric Food Chem 61:103-113.

Alemdar A, Sain M (2008) Isolation and characterization of nanofibers from agricultural residues: Wheat straw and soy hulls. Biores Technol 99:1664-1671.

Awalludin MF, Sulaiman O, Hashim R, Nadhari WNAW (2015) An overview of the oil palm industry in Malaysia and its waste utilization through thermochemical conversion, specifically via liquefaction. Renew Sustain Energy Rev 50:1469-1484.

Azizi Samir MAS, Alloin F, Dufresne A (2005) Review of recent research into cellulosic whiskers, their properties and their application in nanocomposite field. Biomacromolecules 6:612-626.

Bajpai P (2015) Basic overview of pulp and paper manufacturing process. Green chemistry and sustainability in pulp and paper industry. Springer International Publishing, Switzerland. pp 11-39.

Battista OA (1950) Hydrolysis and crystallization of cellulose. Ind Eng Chem 42:502-507.

Bhatia JK, Kaith BS, Kalia S (2016) Recent developments in surface modification of natural fibers for their use in biocomposites. *In* S Kalja, ed. Biodegradable Green Composites. John Wiley & Sons, Inc., Hoboken, NJ. doi:10.1002/9781118911068.ch4.

Behin J, Mikaniki F, Fadaei Z (2008) Dissolving pulp (alpha-cellulose) from corn stalk by kraft process. Iranian Journal of Chemical Engineering 5(3):14-28.

Chan K, Watson I, Lim K (1980) Use of oil palm waste material for increased production [of oil palm, Elaeis guineensis, Jacq., Malaysia]. Conference on Soil Science and Agricultural Development in Malaysia, Kuala Lumpur (Malaysia), 12-14 May 1980, 1980. PSTM.

Elazzouzi-Hafraoui S, Nishiyama Y, Putaux J-L, Heux L, Dubreuil F, Rochas C (2007) The shape and size distribution of crystalline nanoparticles prepared by acid hydrolysis of native cellulose. Biomacromolecules 9:57-65.

FAO, IFAD, IMF, OECD, UNCTAD, WFP, The World Bank, The WTO, IFPRI, UN HLTF (2011) Price volatility in food and agricultural markets: Policy responses. FAO, Rome, Italy.

Fiore V, Scalici T, Di Bella G, Valenza A (2015) A review on basalt fibre and its composites. Compos, Part B Eng 74:74-94.

French AD (2014) Idealized powder diffraction patterns for cellulose polymorphs. Cellulose 21:885-896.

Gurunathan T, Mohanty S, Nayak SK (2015) A review of the recent developments in biocomposites based on natural fibres and their application perspectives. Compos, Part A Appl Sci Manuf 77:1-25.

Haafiz MKM, Eichhorn S, Hassan A, Jawaid M (2013) Isolation and characterization of microcrystalline cellulose from oil palm biomass residue. Carbohydr Polym 93:628-634.

Haafiz MKM, Hassan A, Zakaria Z, Inuwa I (2014) Isolation and characterization of cellulose nanowhiskers from oil palm biomass microcrystalline cellulose. Carbohydr Polym 103:119-125.

Habibi Y, Lucia LA, Rojas OJ (2010) Cellulose nanocrystals: Chemistry, self-assembly, and applications. Chem Rev 110:3479-3500.

Hollaway L (2010) A review of the present and future utilisation of FRP composites in the civil infrastructure with reference to their important in-service properties. Construct Build Mater 24:2419-2445.

Ibrahim MM, El-Zawawy WK, Jüttke Y, Koschella A, Heinze T (2013) Cellulose and microcrystalline cellulose from rice straw and banana plant waste: Preparation and characterization. Cellulose 20:2403-2416.

Ilindra A, Dhake J (2008) Microcrystalline cellulose from bagasse and rice straw. Indian J Chem Technol 15:497-499.

Jagadeesh D, Kanny K, Prashantha K (2015) A review on research and development of green composites from plant protein-based polymers. Polym Compos. doi:10.1002/pc.23718.

Johar N, Ahmad I, Dufresne A (2012) Extraction, preparation and characterization of cellulose fibres and nanocrystals from rice husk. Ind Crops Prod 37:93-99.

Jonoobi M, Mathew AP, Oksman K (2012) Producing low-cost cellulose nanofiber from sludge as new source of raw materials. Ind Crops Prod 40:232-238.

Kalia S, Kaith BS, Kaur I, Njuguna J (2014) Biofiber-reinforced thermoplastic composites. Pages 239-288 in S Thomas, K Joseph, SK Malhotra, K Goda, MS Sreekala, eds. Polymer Composites, Chapter: Biofiber-Reinforced Thermoplastic Composites. Wiley-VCH Verlag GmbH & Co. KGaA. doi:10.1002/9783527674220.ch7.

Khalil HPSA, Bhat A, Yusra AI (2012) Green composites from sustainable cellulose nanofibrils: A review. Carbohydr Polym 87:963-979.

Khalil HPSA, Alwani MS, Omar AKM (2007) Chemical composition, anatomy, lignin distribution, and cell wall structure of Malaysian plant waste fibers. BioResources 1:220-232.

Lionetto F, Del Sole R, Cannoletta D, Vasapollo G, Maffezzoli A (2012) Monitoring wood degradation during weathering by cellulose crystallinity. Materials (Basel) 5:1910-1922.

Mdh B, My R, Ridzuan R, Norhafzan J (2015) Microcrystalline cellulose (MCC) from oil palm empty fruit bunch (EFB) fiber via simultaneous ultrasonic and alkali treatment. Int J Chem Mol Nuc Mat Met Eng 9(1):8-11.

Nagalakshmaiah M, Mortha G, Dufresne A (2016) Structural investigation of cellulose nanocrystals extracted from chili leftover and their reinforcement in cariflex-IR rubber latex. Carbohydr Polym 136:945-954.

Owolabi AWT, Arniza G, Wan Daud W, Alkharkhi AF (2016) Effect of alkaline peroxide pre-treatment on microfibrillated cellulose from oil palm fronds rachis amenable for pulp and paper and bio-composite production. BioResources 11:3013-3026.

Pandey A, Bhaskar T, Stöcker M, Sukumaran R (2015) Recent advances in thermochemical conversion of biomass. Elsevier, Amsterdam, The Netherlands.

Poletto M, Dettenborn J, Pistor V, Zeni M, Zattera AJ (2010) Materials produced from plant biomass. Part I: Evaluation of thermal stability and pyrolysis of wood. Mater Res 13:375-379.

Ramesh M (2016) Kenaf (*Hibiscus cannabinus* L.) fibre based bio-materials: A review on processing and properties. Prog Mater Sci 78:1-92.

Rosa SM, Rehman N, De Miranda MIG, Nachtigall S, Bica CI (2012) Chlorine-free extraction of cellulose from rice husk and whisker isolation. Carbohydr Polym 87:1131-1138.

Sanyang M, Sapuan S, Jawaid M, Ishak M, Sahari J (2016) Recent developments in sugar palm (*Arenga pinnata*) based biocomposites and their potential industrial applications: A review. Renew Sustain Energy Rev 54:533-549.

Segal L, Creely J, Martin A, Conrad C (1959) An empirical method for estimating the degree of crystallinity of native cellulose using the X-ray diffractometer. Textile Research Journal 29:786-794.

Sonia A, Dasan KP (2013) Chemical, morphology and thermal evaluation of cellulose microfibers obtained from *Hibiscus sabdariffa*. Carbohydr Polym 92:668-674.

Sulaiman O, Salim N, Nordin NA, Hashim R, Ibrahim M, Sato M (2012) The potential of oil palm trunk biomass as an alternative source for compressed wood. BioResources 7:2688-2706.

Tye YY, Lee KT, Abdullah WNW, Leh CP (2016) The world availability of non-wood lignocellulosic biomass for the production of cellulosic ethanol and potential pretreatments for the enhancement of enzymatic saccharification. Renew Sustain Energy Rev 60:155-172.

Zahari MW, Hassan OA, Wong H, Liang J (2003) Utilization of oil palm frond-based diets for beef and dairy production in Malaysia. Asian-australas J Anim Sci 16:625-634.

Zeni M, Favero D, Pacheco K, Grisa A (2016) Preparation of microcellulose (Mcc) and nanocellulose (Ncc) from eucalyptus kraft ssp pulp. Polymer Sciences Journal 1:1-7.

Zimniewska M, Wladyka-Przybylak M (2016) Natural fibers for composite applications. *In* Fibrous and Textile Materials for Composite Applications. Springer Science+Business Media, Singapore.